Published in final edited form as:
Circulation. 2011 April 12; 123(14): 1519–1528. doi:10.1161/CIRCULATIONAHA.110.007641.

On T2* Magnetic Resonance and Cardiac Iron

John-Paul Carpenter, MB, MRCP[1,2,*], **Taigang He, PhD**[1,2,*], **Paul Kirk, MB, MRCP**[1,2], **Michael Roughton, MSc**[1,4], **Lisa J Anderson, MD, MRCP**[3], **Sofia V de Noronha, PhD**[1], **Mary N Sheppard, MD, FRCPath**[1], **John B Porter, MD, FRCP, FRCPath**[4], **J Malcolm Walker, FRCP**[4], **John C Wood, MD**[5], **Renzo Galanello, MD**[6], **Gianluca Forni, MD**[7], **Gualtiero Catani, MD**[8], **Gildo Matta, MD**[8], **Suthat Fucharoen, MD**[9], **Adam Fleming, BSc**[10], **Michael J House, PhD**[10], **Greg Black, MSc**[10], **David N Firmin, PhD**[1,2], **Timothy G St. Pierre, PhD**[10], and **Dudley J Pennell, MD, FRCP**[1,2]

[1]Royal Brompton and Harefield NHS Foundation Trust, London, UK [2]National Heart and Lung Institute, Imperial College London, UK [3]St George's Hospital NHS Trust, London, UK [4]University College Hospitals NHS Trust, London, UK [5]Children's Hospital Los Angeles, California, USA [6]Università degli Studi di Cagliari, Ospedale Regionale Microcitemie, Cagliari, Italy [7]Ospedali Galliera di Genova, Genoa, Italy [8]Azienda Ospedaliera Brotzu, Cagliari, Italy [9]Mahidol University, Puttamonthon Nakornpathom, Thailand [10]The University of Western Australia, Perth, Australia

Abstract

Background—Measurement of myocardial iron is key to the clinical management of patients at risk of siderotic cardiomyopathy. The cardiovascular magnetic resonance (CMR) relaxation parameter R2* (assessed clinically via its reciprocal T2*) measured in the ventricular septum is used to assess cardiac iron, but iron calibration and distribution data in humans is limited.

Methods and Results—Twelve human hearts were studied from transfusion dependent patients following either death (heart failure n=7, stroke n=1) or transplantation for end-stage heart failure (n=4). After CMR R2* measurement, tissue iron concentration was measured in multiple samples of each heart using inductively coupled plasma atomic emission spectroscopy. Iron distribution throughout the heart showed no systematic variation between segments, but epicardial iron concentration was higher than in the endocardium. The mean (±SD) global myocardial iron causing severe heart failure in 10 patients was 5.98 ±2.42mg/g dw (range 3.19–9.50), but in 1 outlier case of heart failure was 25.9mg/g dw. Myocardial ln[R2*] was strongly linearly correlated with ln[Fe] (R^2=0.910, p<0.001) leading to $[Fe]=45.0\bullet(T2^*)^{-1.22}$ for the clinical calibration equation with [Fe] in mg/g dw and T2* in ms. Mid-ventricular septal iron concentration and R2* were both highly representative of mean global myocardial iron.

Corresponding author: Dr John-Paul Carpenter, Royal Brompton and Harefield NHS Trust, Sydney Street, London, SW3 6NP, United Kingdom, Tel: +44 20 7351 8800, Fax: +44 20 7351 8816, J.Carpenter@rbht.nhs.uk.
*These authors contributed equally to this article

The other authors report no conflicts.

Disclosures

Dr Carpenter has received honoraria from Novartis, Apotex and Swedish Orphan. Dr He is supported by the British Heart Foundation and is a consultant to Novartis. Professor Porter has received research funding from and served on the speakers' bureau and advisory board for Novartis. Professor Galanello served on the speakers' bureau for Novartis and ApoPharma. Dr Forni has received research funding from Novartis. Professor Fucharoen is a Senior Research Scholar of the Thailand Research Fund. Professor Firmin has received research support from Siemens. Professor Pennell is a consultant to and served on advisory boards and speakers' bureau for Novartis, ApoPharma and Siemens; has received research funding from Novartis; and is a director and stockholder for Cardiovascular Imaging Solutions. Professor St Pierre holds shares in and is on the Board of Directors of Resonance Health Ltd, and has received research funding from Novartis. Professor Wood has received research funding from Novartis and is a consultant for Ferrokin Biosciences.

Conclusions—These data detail the iron distribution throughout the heart in iron overload and provide calibration in humans for CMR R2* against myocardial iron concentration. The iron values are of considerable interest with regard to the level of cardiac iron associated with iron-related death and indicate that the heart is more sensitive to iron loading than the liver. The results also validate the current clinical practice of monitoring cardiac iron in-vivo by CMR of the mid septum.

Keywords

Magnetic resonance imaging; heart; iron overload; siderosis; thalassemia

Introduction

Transfusion-dependent patients receive approximately 20 times the normal intake of iron which leads to iron accumulation and damage in the liver, heart and endocrine organs.[1,2] Although improvements in survival have been achieved over the last 40 years, iron induced cardiotoxicity remains a leading cause of morbidity and mortality, especially for patients with beta thalassemia major (TM),[3,4,5,6] and once heart failure develops, the prognosis is poor.[7] Therefore, assessment of myocardial iron is essential clinically but conventional non-invasive techniques are less than ideal. Neither serum ferritin nor liver iron concentration gives a reliable indication of cardiac iron in cross-sectional studies.[8] Monitoring ejection fraction can be useful, but its value is limited by difficulty of reproducible longitudinal measurements, the masking of ventricular dysfunction by the basal high cardiac output seen in chronic anemia, and its late occurrence in the disease process. Even more modern contractile measures such as tissue Doppler imaging correlate poorly with cardiac iron.[9] Endomyocardial biopsy is also unreliable for measuring myocardial iron due to sampling error with very small biopsy samples.[10,11] The need for an alternative non-invasive measurement of myocardial iron led to the development of an optimized cardiac T2* magnetic resonance (MR) technique. Particulate intracellular iron causes shortening of the magnetic resonance relaxation parameter T2* (and hence increase in its reciprocal, R2*) due to microscopic magnetic field inhomogeneity. Myocardial T2* is an easily quantifiable, clinically robust and highly reproducible measurement technique.[12,13,14] In the liver, T2* correlates well with biopsy iron concentration.[8,15] Although the relationship between T2* and cardiac iron can be inferred from first principles, animal models,[16] and the liver data, there is limited direct information on cardiac calibration of T2* in humans,[17,18] and the inherent limitations associated with endomyocardial biopsy prevent in vivo calibration.[19] We therefore initiated a project to calibrate cardiac T2* against chemically assayed tissue iron concentration in ex-vivo human hearts and determine its cardiac distribution.

Methods

Patient characteristics

This project started in 2003 and was completed in 2010, during which time 12 whole human hearts were donated from five international centres: University College Hospital (London, UK), Ospedale Galleria (Genoa, Italy), Children's Hospital of Los Angeles (USA), Azienda Ospedaliera Brotzu (Cagliari, Italy) and Mahidol University (Bangkok, Thailand). All patients were transfusion-dependent (10 beta-thalassemia major, 1 sideroblastic anemia, 1 Diamond Blackfan anemia), most having required transfusions from early childhood. The hearts were donated following death or cardiac transplantation for end-stage heart failure. The study protocol was approved by all local research ethics committees, and local consent was obtained in all cases.

Imaging protocol and analysis

We used scientific convention in quoting R2* to evaluate relaxation and its relation to iron, R2* being the reciprocal of T2*. Scans performed on patients pre-mortem are quoted as T2*. All hearts were fixed in formalin. Each heart was cut into 4–5 slices of 1cm thickness in the ventricular short axis according to ventricular size (figure 1a,b). The apical cap was not analyzed for R2* because of potential for partial volume effects. All slices were imaged using a 1.5 Tesla MR scanner (Sonata, Siemens Medical Systems, Germany) with a 4-element phased-array coil. Slices were immersed in water in a custom-made container between two sheets of plexiglass and maintained at 37°C throughout imaging (figure 1c). A multi-echo gradient echo sequence was used for imaging, and in order to cover R2* values from 25 to 500s^{-1} (T2* from 2 to 40ms), 2 sequences were required. For all hearts, a high resolution sequence with 16 echoes was used with TEs from 3.1 to 39.1ms. Slice thickness was 5mm, flip angle 35°, matrix 128×128 pixels, field of view 160mm, number of excitations 2 and sampling bandwidth 815Hz per pixel. An additional lower resolution sequence with a lower minimum TE was also performed with 12 echoes ranging from 1.21 to 14.9ms. For this sequence, flip angle was 20°, matrix 64×64 pixels and sampling bandwidth 1955Hz per pixel. All other parameters were identical. The 2 sequences were compared in 6 ex-vivo hearts with a range of R2* from 125 to 278s^{-1} (T2* from 3.6 to 8.0ms), and found to agree closely with a coefficient of variation of 5.1%. Care was taken to orientate each slice, including photography, to ensure reliable identification of anatomy and wall segmentation for co-localization of R2* and chemically assayed iron concentration.

For the measurement of R2*, each slice was analyzed with 18 regions of interest (ROIs) of 6 radial sectors of 60° each, and 3 layers: outer (epicardial), inner (endocardial) and intermediate (mesocardial) (figure 1d). The attachment of the right ventricular (RV) wall to the left ventricle (LV) was used to define the septum.[20] R2* was measured from each ROI using dedicated software (Thalassaemia Tools, Cardiovascular Imaging Solutions, London) using a truncation model to account for background noise, as has been previously validated (figure 2).[21] Analysis of the 12 echo sequence was only required for heart 4, which was extremely heavily iron loaded (R2* 500s^{-1}, T2* 2.0ms). In all other cases, the 16 echo sequence was used for analysis.

Quantification of myocardial iron

After R2* CMR was completed, each short axis slice was cut into 6 sectors of 60° each, and then each sector was subdivided into 3 transmural layers (18 LV samples, figure 1e). For each short axis slice, 2 samples were also taken from the RV free wall (20 myocardial samples per slice). Additional samples were taken from the right (3) and left (3) atrium, the inter-atrial septum (1) and each of the valves (4). For the LV myocardial R2* calibration analysis, all LV samples were directly compared with the CMR R2* scan. For the segmental analysis of the distribution of myocardial iron, we used the American Heart Association/ American College of Cardiology (AHA/ACC) 16-segment model.[20] Three myocardial slices from each heart were used for this analysis: the mid-ventricular, apical and basal slices, as per the model. Each segment comprised the full transmural extent of myocardium. To match the apical slice to 4 segments as dictated in the 16 segment model, the 2 apical-septal sectors were analyzed together, and the 2 apical-lateral sectors were analyzed together. The wet weight of each piece of tissue was recorded after discarding excess formalin. Samples were then freeze-dried and the dry weight (dw) was recorded immediately after removal from the lyophilizer. Following acid digestion, iron measurement was performed using inductively coupled plasma atomic emission spectroscopy (ICP-AES). The iron concentrations in samples of NIST human liver standard 4352 were used as quality controls for ICP-AES analysis.

Effect of time in formalin fixation on R2* measurement and iron concentration

As the fixed hearts had been stored for varied lengths of time, the effect of formalin on MR relaxation and iron loss over time was studied. One myocardial slice was analysed at repeated intervals up to a total of 566 days (12 scans in total). Myocardial tissue from an apical slice not included in the segmental analysis was used to assess whether there was any leaching of iron from the myocardium into formalin over time. This 7.35g sample was preserved in 280mL of 10% neutral buffered formalin (pH 7.0). At repeated intervals up to 600 days, small (1mL) aliquots of formalin were taken for analysis of the iron content of the solution. The initial iron concentration in this tissue sample was estimated from immediately adjacent areas of myocardium in the same apical slice.

Pre and post-mortem scans

Three of the patients had clinical T2* scans shortly before death on the same scanner (Sonata) as was used for the ex-vivo scanning. Imaged was performed with a single breath-hold 8-echo T2* sequence as previously described (range of echo times: 2.6–16.74ms, slice thickness 10mm, flip angle 20°, matrix 128×256 pixels, field of view 400mm, sampling bandwidth 815Hz per pixel).[13] The anatomical appearance of the slice (papillary muscle position, trabecular pattern and distance from apex) was used to achieve as precise a correlation as possible between pre- and post-mortem scans, allowing direct comparison of T2* values. Two mid-ventricular short-axis slices were imaged, which gave 12 myocardial regions of interest for comparison (2 slices, 2 septal sectors, 3 transmural layers).

Statistics

For each distribution analysis, 1 region of interest was defined as the reference region, and differences in tissue iron content throughout the heart against this region were assessed using mixed-model linear regression. The null hypothesis was that there was no difference in iron concentration between segments, layers or slices. For each analysis, the regions of interest were entered as fixed effects, so that differences between regions could be estimated. Patients were entered as random effects, since it was not of interest to test for differences between individual patients. To account for the repeated measurements from each heart, all samples from each individual heart were nested for analysis. R2* was compared with iron concentration using linear regression. The degree of heterogeneity of iron concentration and R2* for each heart was evaluated by calculating the coefficient of variation of iron concentration across all samples. All data were analysed using STATA version 10.1 (StataCorp, Texas, USA). Mixed model linear regression analysis was performed using the “xtmixed” command within STATA. The “regress” command was used when performing standard linear regression. A value of $P < 0.05$ was used to define a significant difference.

Results

Patient characteristics

Twelve hearts were donated, 8 following death and 4 from patients undergoing cardiac transplantation for end-stage heart failure. End-stage heart failure was the cause of death in 7 of the 8 patients who died, but one patient died from an ischemic stroke at the age of 46 with a history of excellent compliance to chelation therapy and no cardiac complications (apart from a transient episode of atrial fibrillation aged 21). Table 1 summarises the clinical information for each patient.

Pre and post-mortem scans

Three patients underwent both pre- and post-mortem T2* scans. The mean time between CMR scan and death was 26 ±13.3 days (range 11–35). There was no significant difference in T2* between scans. Mean ±SD T2* pre-mortem was 4.89 ±1.30, 6.01 ±0.81 and 10.87 ±2.34ms versus 5.21 ±0.43ms (P=0.28), 5.94 ±0.90ms (P=0.84) and 9.20 ±2.22ms (P=0.21) post-mortem for pairwise comparison of the septal regions of interest in hearts 2, 10 and 11 respectively (figure 3a, b, c).

Effect of time in formalin on R2* measurement

For the single short axis slice which was scanned at repeated intervals, there was no significant change in R2* value, even after 18 months' storage in formalin (figure 3d). Mean R2* for all sectors was 198.4 ±21.5s^{-1} at day 6 and 197.7 ±7.3s^{-1} at day 566 (P=0.93).

Loss of iron from stored myocardial samples

The iron content of the formalin solution in which a piece of myocardial tissue had been stored over a period of 600 days is shown in figure 3e. Average iron concentration of adjacent myocardial tissue was 1.21 mg/g wet weight, corresponding to a total of 8.91mg of iron in the 7.35g wet weight sample. The iron concentration of the solution increased rapidly over the first 30 days after formalin fixation, with a further subsequent rise but thereafter stabilised to reach a plateau of approximately 480μg/L after 300 days, equating to a loss of 135μg (approximately 1.5%) of the total iron from the myocardial tissue.

Myocardial iron samples: overall summary

The mean (± SD) weight of all samples in the iron analysis was 1001 ±620mg. Iron concentration in all samples ranged from 0.09 to 78.64mg/g dw. The myocardial iron concentration ranged from 0.18 to 53.4mg/g dw. The mean (± SD) ratio of dry to wet iron concentration in the myocardium was 5.04 ±0.9 and was independent of iron concentration. One heart had exceptionally high levels of iron and in view of the possibility that this could bias the results, all further analysis is presented separately for this outlier heart. The coefficient of variation of iron for myocardial samples ranged from 9.2% to 26.6% per heart with a mean of 15.2% (table 1).

Distribution of left ventricular iron

With all hearts considered together (except the most heavily iron-loaded heart (number 4), a gradient of iron was found in the transmural layers of the LV myocardium with the greatest concentration in the epicardium, an intermediate level in the mesocardium (−1.1%, p=0.63), and the lowest level in the endocardium (−7.5%, p=0.001) (figure 4a and table 2). No statistically significant systematic variations in iron concentration were observed between the different AHA segments. In order to examine for variation in larger regions of the LV, an analysis was also performed of variation in iron concentration of whole walls of the LV (inferoseptal, anteroseptal, anterior, anterolateral, inferolateral, inferior) encompassing all segments from base to apex, which again showed no significant systematic variation of mean iron concentration. A further analysis comparing the whole basal, mid-ventricular and apical slices also failed to show any significant systematic variation in mean iron concentration. The most heavily iron-loaded heart (heart 4) had very high iron concentration in the epicardium (36.1mg/g dw) with an intermediate level in the endocardium (−28.0%) and the lowest level in the mesocardium (−54.7%) (figure 4a and table 2). There was no systematic variation in mean iron concentration between the different LV segments or from base to apex.

Septal iron compared with global cardiac iron

Iron concentration measured in the mid-septal slice was highly representative of global iron (figure 4b). Regression analysis showed a slope indistinguishable from 1 (1.06; 95% CI: 0.83 to 1.29) and an intercept indistinguishable from 0 (0.04; 95% CI: −1.57 to 1.66). The mean percentage (±SD) difference between mid-septal and global iron concentration was 10.5 ±13.4%.

Distribution of iron in RV, atria and valves

Excluding the most heavily iron-loaded heart (heart 4), all RV, atrial and valve samples showed lower iron levels compared to global LV iron (apart from the anterior left atrial wall where only a borderline difference was observed). The RV wall had up to 21.9% less iron ($p<0.001$). Compared to the mean global LV iron concentration, the left atrial iron concentration was up to 28.1% lower ($p<0.001$) and right atrial iron up to 57.0% lower ($p<0.001$). All 4 cardiac valves showed low iron concentrations which were up to 74.4% lower than the LV ($p<0.001$). Heart 4 showed a consistently higher level of iron in the atrial and valve samples but no difference between LV and RV iron (table 3).

Relation of R2* to tissue iron concentration

Due to the very high level of iron in the most severely overloaded heart (heart 4), measurement of R2* might be underestimated. Therefore, the results of the MR relaxation calibration are presented twice, both including and then excluding this heart. A total of 1006 tissue samples and their corresponding ROIs were used for iron and R2* assessment, with 84 ROIs (8.3%) being excluded from the R2* analysis due to imaging artefact predominantly caused by cuts made at autopsy. A curvilinear relation between R2* and cardiac iron concentration was observed (Figure 5a,b). A similar curvilinear relation was shown when mean global whole heart iron was plotted against R2* (figure 5c,d). The strongest linear correlation was found (all hearts) by plotting lnR2* and ln[Fe] (R^2 0.910, $p<0.001$) with a slope of 0.745 [95% CI: 0.729–0.760] and intercept of 3.896 [95% CI: 3.868–3.924] (figure 5e). There was almost no difference to this calibration result if heart 4 was excluded (R^2 0.898, $p<0.001$, slope 0.754 [95% CI: 0.737–0.772], intercept 3.884 [95% CI: 3.855–3.913]). Using this calibration in all hearts, the relation between R2* and iron is expressed by the formula (where myocardial [Fe] is measured in mg/g dw, and R2* is measured in s^{-1}):

$$[\mathrm{Fe}]=0.00985 \bullet (R2^{*})^{1.22}$$

R2* measured in the mid-septal slice was highly representative of whole-heart mean R2* (figure 5f). Regression analysis showed a slope indistinguishable from 1 (0.97; 95% CI: 0.82 to 1.13) and an intercept indistinguishable from 0 (0.33; 95% CI: −0.73 to 1.38). The mean percentage (±SD) difference between mid-septal and global R2* was 2.8 ±7.3%. The relation of septal R2* and T2* with whole heart iron concentration is shown in figure 6.

Discussion

This is the first report of a series of human hearts that have undergone both magnetic resonance relaxometry and quantitative iron studies for distribution and calibration purposes. The results of the distribution analysis show no systematic variation of iron concentration between all 16 myocardial segments, the 6 myocardial walls, or the 3 short axis slices from base to apex. However, systematically higher iron concentration was present in the epicardium. The mid-ventricular septal iron concentration was highly representative of global iron concentration, and mid-ventricular R2* was highly representative of global R2*.

Studies dating from the mid-1950s have assessed myocardial iron loading in post-mortem human hearts using various techniques including histological grading of iron-positive myocytes, electron microscopy and analysis of elemental iron by flameless atomic absorption spectroscopy.[11,22,23,24,25,26,27] Our results are in broad agreement with the previously published studies which have observed a similar transmural gradient of myocardial iron. Two autopsy studies have attempted to quantify regional variation but no definite pattern has emerged,[17,22] and this is the first time a comprehensive study of regional variation has been made.

CMR studies have reported that some TM patients have a heterogeneous pattern of cardiac iron distribution, as measured by in vivo T2*, although this heterogeneity lessened with increasing iron concentration.[28,29] Myocardial T2* in vivo may however be confounded by a number of factors, including magnetic susceptibility artefact as well as measurement error.[30] In view of the problems with artefact in-vivo, it has been recommended that the measurement of T2* is restricted to a full thickness septal region of interest.[8] There has been recent debate over the use of this septal ROI for predicting whole-heart iron,[29] but our results validate this approach given that both iron and R2* measured in the mid-septum are highly representative of their respective global myocardial value.

The results of the calibration analysis of myocardial MR relaxometry against absolute iron concentration are of considerable clinical interest. Heart R2* provided a robust (R^2=0.910) calibration against chemically assayed cardiac iron in the current study. Our statistical analysis demonstrated that this relationship was curvilinear. Previous investigators have described a linear relationship between R2* and iron concentration, but these studies had fewer observations and a more limited range of measurement.[17] Although R2* underestimation may occur at high iron concentrations if initial echo times are too long, a minimum echo time of 1.2ms should have been adequate to capture even the most heavily loaded samples. In addition, we found little calibration differences if heart 4 was included or excluded. For clinical purposes, where T2* is typically the result quoted for patients with suspected cardiac iron overload, the calibration equation can be rewritten using T2* = 1000/R2* when the units of T2* are expressed in ms, and R2* in s^{-1}:

$$[\mathrm{Fe}]=45.0 \bullet (T2^{*})^{-1.22}$$

Although direct comparison across species should be treated with caution, our results are comparable with R2* measurements in a gerbil model of severe iron loading where tissue iron concentration was measured from fresh, unfixed tissue.[16] Proton relaxivity is known to be temperature dependent and in phantom studies, T2* falls by up to 1.5% per degree Celsius.[31] We scanned all hearts at a constant 37°C and this may account for the consistency of our pre and post-mortem heart measurements. The hearts in this study had been stored in formalin and there was a concern that this could affect the measurement of T2* and iron concentration. In agreement with previous work, we found only minor leaching of iron from myocardial tissue into the formalin solution and very little variation in the measured T2* over time.[32]

The iron values obtained from our study are of considerable interest with regard to the level of cardiac iron concentration which is associated with iron-related death and cardiac disease, an issue that has hitherto been little explored. One previous study reported the normal myocardial iron concentration to be 0.34 (range 0.29–0.47) mg/g dw.[33] The one heart we studied from a patient who died of a stroke with no evidence of heart disease and a normal myocardial T2*, had a global iron concentration of 0.38mg/g dw, which is in good agreement with the previous study. Of 10 hearts with similar ranges of myocardial siderosis,

the mean global myocardial iron causing severe heart failure was 5.98 ±2.42mg/g dw (range 3.19–9.50), but in 1 outlier case of heart failure, myocardial iron was 25.9mg/g dw. The values seen in the 10 hearts are rather modest in comparison with iron levels commonly seen in the liver in TM, and this indicates that the heart is considerably more sensitive to iron loading than the liver in terms of functional consequences. The outlier heart had 5 times the iron concentration compared to the mean value of the other hearts, which was a totally unexpected finding. The explanation for this tolerance to myocardial iron can only be speculative, but may have been genetically mediated.

Also of interest is the myocardial T2* value in relation to the development of heart failure and death. Previous ranges for T2* in vivo have been derived solely from clinical observations. In normal volunteers with no history of blood transfusion or iron overload, Anderson's first paper on myocardial T2* found a mean normal value of 52ms,[8] which yields a myocardial iron concentration of 0.36mg/g dw from our calibration. More recently, a normal mean value of 40ms has been widely used which equates to 0.50mg/g dw. These values accord well with the previous published normal values for myocardial iron,[33] and also with the global myocardial T2* value (44.4ms) of one patient in our study who died of a stroke. The myocardial T2* values associated with being below the normal range are typically those below 20ms (1.1 mg/g dw), and as T2* falls below 10ms (2.7mg/g dw), there is a progressive decline in both LV and RV ejection fraction.[8,34] The vast majority of patients who present with heart failure due to cardiac iron overload have T2* <10ms and low T2* values are powerful independent predictors of subsequent development of cardiac failure.[35] All but one of the hearts in this study were from patients who had either died from or had undergone cardiac transplantation for end-stage heart failure. In keeping with clinical experience, the mean myocardial T2* was 5.9 ±3.0ms (range 2.0–12.3).

Limitations

This project has required international collaboration between specialist centres and could not have been performed with fresh, unfixed hearts due to regulations on transport of human tissue between sites. The fact that death from cardiac failure is almost always restricted to patients with severe cardiac iron loading (T2* <10ms) is reflected in the range of T2* values. Although there is no guarantee that in-vivo and ex-vivo myocardial T2* are the same, the data are supportive with a good agreement between pre- and post-mortem T2* values in 3 hearts. Some hearts had been stored in formalin over extended periods, but our data suggest that there is no significant change in T2* over time and only a small amount of leaching of iron into the formalin solution. Although every effort was made to correlate ROIs used for R2* measurement with the tissue blocks that were analysed for iron concentration, it is not possible to eliminate disparity completely There are difficulties with R2* measurement in heavily iron-loaded tissue where signal decay is rapid, requiring very short echo times. Scanner hardware imposes constraints on minimum echo spacing which may be inadequate for accurate R2* measurement at very high iron concentrations. However, a minimum echo time of 1.2ms should allow reliable measurement of T2* values as low as 1.44ms,[16] which is below the minimum global myocardial value seen in this study. Finally, some ROIs were excluded from the calibration due to imaging artefact. The decision to exclude an ROI was made by subjective assessment prior to the analysis of R2* and is unlikely to have affected the calibration significantly due to the many regions sampled throughout the 12 hearts. Previous reports have examined the myocardial relaxation parameter T2 in relation to cardiac iron in animal models,[36] and in humans.[16,19] T2 imaging can be challenging however, and it is not in routine clinical use, although recent imaging advances have been made.[37] Due to the ease of acquisition and robust nature of T2* for clinical practice, we have concentrated on this technique.

Conclusions

The results of the current study validate the clinical technique in current use, and provide detailed calibration and distribution data in humans.

Acknowledgments

We are indebted to the generosity of the patients and families without whose help we would have been unable to perform this important study. We would like to thank Steven Collins for assistance in scanning the ex-vivo hearts and Cathleen Enriquez for her assistance in preparing this manuscript.

Sources of Funding

This work was supported by the NIHR Cardiovascular Biomedical Research Unit at the Royal Brompton and Harefield NHS Foundation Trust and Imperial College London. Financial support was also received from the National Institutes of Health through grant number R01 DK066084-01 and from the Australian Research Council through grant number DP0985848.

References

1. Gordeuk VR, Bacon BR, Brittenham GM. Iron overload: causes and consequences. Ann Rev Nutr. 1987; 7:485–508. [PubMed: 3300744]
2. McLaren GD. Iron overload disorders: Natural history, pathogenesis, diagnosis, and therapy. Crit Rev Clin Lab Sci. 1983; 19:205–66. [PubMed: 6373141]
3. Borgna-Pignatti C, Rugolotto S, De Stefano P, Piga A, Di Gregorio F, Gamberini MR, Sabato V, Melevendi C, Cappellini MD, Verlato G. Survival and disease complications in thalassemia major. Ann NY Acad Sci. 1998; 850:227–31. [PubMed: 9668544]
4. Modell B, Khan M, Darlison M. Survival in beta thalassaemia major in the UK: data from the UK Thalassaemia Register. Lancet. 2000; 355:2051–2. [PubMed: 10885361]
5. Modell B, Khan M, Darlison M, Westwood MA, Ingram D, Pennell DJ. Improved survival of thalassaemia major in the UK and relation to T2* cardiovascular magnetic resonance. J Cardiovasc Magn Reson. 2008; 10:42. [PubMed: 18817553]
6. Borgna-Pignatti C, Rugolotto S, De Stefano P, Zhao H, Cappellini MD, Del Vecchio GC, Romeo MA, Forni GL, Gamberini MR, Ghilardi R, Piga A, Cnaan A. Survival and complications in patients with thalassemia major treated with transfusion and deferoxamine. Haematologica. 2004; 89:1187–93. [PubMed: 15477202]
7. Felker GM, Thompson RE, Hare JM, Hruban RH, Clemetson DE, Howard DL, Baughman KL, Kasper EK. Underlying causes and long-term survival in patients with initially unexplained cardiomyopathy. N Engl J Med. 2000; 342:1077–84. [PubMed: 10760308]
8. Anderson LJ, Holden S, Davis B, Prescott E, Charrier CC, Bunce NH, Firmin DN, Wonke B, Porter J, Walker JM, Pennell DJ. Cardiovascular T2-star (T2*) magnetic resonance for the early diagnosis of myocardial iron overload. Eur Heart J. 2001; 23:2171–9. [PubMed: 11913479]
9. Leonardi B, Margossian R, Colan SD, Powell AJ. Relationship of magnetic resonance imaging estimation of myocardial iron to left ventricular systolic and diastolic function in thalassemia. JACC Cardiovasc Imaging. 2008; 1:572–8. [PubMed: 19356483]
10. Fitchett DH, Coltart DJ, Littler WA, Leyland MJ, Trueman T, Gozzard DI, Peters TJ. Cardiac involvement in secondary haemochromatosis: a catheter biopsy study and analysis of myocardium. Cardiovascular Research. 1980; 14:719–24. [PubMed: 7260965]
11. Olson LJ, Edwards WD, Holmes DR Jr, Miller FA Jr, Nordstrom LA, Baldus WP. Endomyocardial biopsy in hemochromatosis: clinicopathologic correlates in six cases. J Am Coll Cardiol. 1989; 13:116–20. [PubMed: 2909558]
12. Westwood MA, Anderson LJ, Firmin DN, Gatehouse PD, Lorenz CH, Wonke B, Pennell DJ. Interscanner reproducibility of cardiovascular magnetic resonance T2* measurements of tissue iron in thalassemia. J Magn Reson Imaging. 2003; 18:616–20. [PubMed: 14579406]

13. Westwood M, Anderson LJ, Firmin DN, Gatehouse PD, Charrier CC, Wonke B, Pennell DJ. A single breath-hold multiecho T2* cardiovascular magnetic resonance technique for diagnosis of myocardial iron overload. J Magn Reson Imaging. 2003; 18:33–9. [PubMed: 12815637]

15. Wood JC, Enriquez C, Ghugre N, Tyzka JM, Carson S, Nelson MD, Coates TD. MRI R2 and R2* mapping accurately estimates hepatic iron concentration in transfusion-dependent thalassemia and sickle cell disease patients. Blood. 2005; 106:1460–5. [PubMed: 15860670]

16. Wood JC, Otto-Duessel M, Aguilar M, Nick H, Nelson MD, Coates TD, Pollack H, Moats R. Cardiac iron determines cardiac T2*, T2, and T1 in the gerbil model of iron cardiomyopathy. Circulation. 2005; 112:535–43. [PubMed: 16027257]

17. Ghugre NR, Enriquez CM, Gonzalez I, Nelson MD Jr, Coates TD, Wood JC. MRI detects myocardial iron in the human heart. Magn Reson Med. 2006; 56:681–6. [PubMed: 16888797]

18. Wang ZJ, Fischer R, Chu Z, Mahoney DH Jr, Mueller BU, Muthupillai R, James EB, Krishnamurthy R, Chung T, Padua E, Vichinsky E, Harmatz P. Assessment of cardiac iron by MRI susceptometry and R2* in patients with thalassemia. Magn Reson Imaging. 2010; 28:363–71. [PubMed: 20061110]

19. Mavrogeni SI, Markussis V, Kaklamanis L, Tsiapras D, Paraskevaidis I, Karavolias G, Karagiorga M, Douskou M, Cokkinos DV, Kremastinos DT. A comparison of magnetic resonance imaging and cardiac biopsy in the evaluation of heart iron overload in patients with beta-thalassemia major. Eur J Haematol. 2005; 75:241–7. [PubMed: 16104881]

20. Cerqueira MD, Weissman NJ, Dilsizian V, Jacobs AK, Kaul S, Laskey WK, Pennell DJ, Rumberger JA, Ryan T, Verani MS. Standardized myocardial segmentation and nomenclature for tomographic imaging of the heart: a statement for healthcare professionals from the Cardiac Imaging Committee of the Council on Clinical Cardiology of the American Heart Association. Circulation. 2002; 105:539–42. [PubMed: 11815441]

21. He T, Gatehouse PD, Kirk P, Mohiaddin RH, Pennell DJ, Firmin DN. Myocardial T2* measurement in iron-overloaded thalassemia: an ex vivo study to investigate optimal methods of quantification. Magn Reson Med. 2008; 60:350–6. [PubMed: 18666131]

22. Olson LJ, Edwards WD, McCall JT, Ilstrup DM, Gersh BJ. Cardiac iron deposition in idiopathic hemochromatosis: histologic and analytic assessment of 14 hearts from autopsy. J Am Coll Cardiol. 1987; 10:1239–43. [PubMed: 3680791]

23. Engle MA, Erlandson M, Smith CH. Late cardiac complications of chronic, severe, refractory anemia with hemochromatosis. Circulation. 1964; 30:698–705. [PubMed: 14226168]

24. Schellhammer PF, Engle MA, Hagstrom JW. Histochemical studies of the myocardium and conduction system in acquired iron-storage disease. Circulation. 1967; 35:631–7. [PubMed: 6024007]

25. James TN. Pathology of the cardiac conduction system in hemochromatosis. N Engl J Med. 1964; 271:92–4. [PubMed: 14149262]

26. Buja LM, Roberts WC. Iron in the heart. Etiology and clinical significance. Am J Med. 1971; 51:209–21. [PubMed: 5095527]

27. Kyriacou K, Michaelides Y, Senkus R, Simamonian K, Pavlides N, Antoniades L, Zambartas C. Ultrastructural pathology of the heart in patients with beta-thalassaemia major. Ultrastruct Pathol. 2000; 24:75–81. [PubMed: 10808552]

28. Positano V, Pepe A, Santarelli MF, Ramazzotti A, Meloni A, De Marchi D, Favilli B, Cracolici E, Midiri M, Spasiano A, Lombardi M, Landini L. Multislice multiecho T2* cardiac magnetic resonance for the detection of heterogeneous myocardial iron distribution in thalassaemia patients. NMR Biomed. 2009; 22:707–15. [PubMed: 19322807]

29. Pepe A, Positano V, Santarelli MF, Sorrentino F, Cracolici E, De Marchi D, Maggio A, Midiri M, Landini L, Lombardi M. Multislice multiecho T2* cardiovascular magnetic resonance for detection of the heterogeneous distribution of myocardial iron overload. J Magn Reson Imaging. 2006; 23:662–8. [PubMed: 16568436]

30. Wacker CM, Bock M, Hartlep AW, Beck G, van Kaick G, Ertl G, Bauer WR, Schad LR. Changes in myocardial oxygenation and perfusion under pharmacological stress with dipyridamole: assessment using T2* and T1 measurements. Magn Reson Med. 1999; 41:686–95. [PubMed: 10332843]

31. He T, Smith G, Carpenter JP, Mohiaddin R, Pennell DJ, Firmin D. A phantom study of temperature-dependent MRI T2* measurement. J Cardiovasc Magn Reson. 2009; 11(Suppl 1):P147.

32. Chua-anusorn W, Webb J, Macey DJ, Pootrakul P, St Pierre TG. The effect of histological processing on the form of iron in iron-loaded human tissues. Biochim Biophys Acta. 1997; 1360:255–61. [PubMed: 9197468]

33. Collins W, Taylor WH. Determination of iron in cardiac and liver tissues by plasma emission spectroscopy. Ann Clin Biochem. 1987; 24:482–7.

34. Alpendurada F, Carpenter JP, Deac M, Kirk P, Walker JM, Porter JB, Banya W, He T, Smith GC, Pennell DJ. Relation of myocardial T2* to right ventricular function in thalassaemia major. Eur Heart J. 2010; 31:1648–54. [PubMed: 20413399]

35. Kirk P, Roughton M, Porter JB, Walker JM, Tanner MA, Patel J, Wu D, Taylor J, Westwood MA, Anderson LJ, Pennell DJ. Cardiac T2* magnetic resonance for prediction of cardiac complications in thalassemia major. Circulation. 2009; 120:1961–8. [PubMed: 19801505]

36. Liu P, Henkelman M, Joshi J, Hardy P, Butany J, Iwanochko M, Clauberg M, Dhar M, Mai D, Waien S, Olivieri N. Quantification of cardiac and tissue iron by nuclear magnetic resonance relaxometry in a novel murine thalassaemia-cardiac iron overload model. Can J Cardiol. 1996; 12:155–164. [PubMed: 8605637]

37. He T, Gatehouse PD, Anderson LJ, Tanner M, Keegan J, Pennell DJ, Firmin DN. Development of a novel optimized breathhold technique for myocardial T2 measurement in thalassemia. J Magn Reson Imaging. 2006; 24:580–5. [PubMed: 16892203]

Commentary

Measurement of myocardial iron is key to the clinical management of patients at risk of iron-overload cardiomyopathy, which is a major killer in transfusion-dependent patients and others with errors of iron metabolism. This especially applies to the large cohort of beta thalassemia major patients, in whom iron accumulation leads to damage in the liver, heart and endocrine organs. Myocardial iron is assessed clinically using the cardiovascular magnetic resonance (CMR) relaxation parameter T2*. This study describes the calibration of CMR relaxation against human iron concentration, and also the iron distribution throughout the heart under conditions of iron overload. A strong correlation was observed between CMR relaxation measurements and biochemically derived tissue iron concentration in 12 postmortem human hearts from transfusion dependent patients, leading to a clinical calibration equation of $[Fe] = 45.0 \bullet (T2^*)^{-1.22}$ where [Fe] is measured in mg/g dry weight and T2* is measured in ms. There was no systematic variation iron concentration throughout the heart, but higher iron levels were found in the epicardium than the endocardium. The data also show that CMR measurements in the mid-ventricular septum are very representative of whole-heart iron concentration, which validates the current clinical approach which is in widespread use. These data show that T2* CMR can be used to measure myocardial iron, and validate its use as an endpoint in clinical trials for improvement of efficacy of cardiac iron chelation treatment to prevent heart failure and death. This will significantly impact the healthcare of the many thousands of transfusion-dependent patients worldwide.

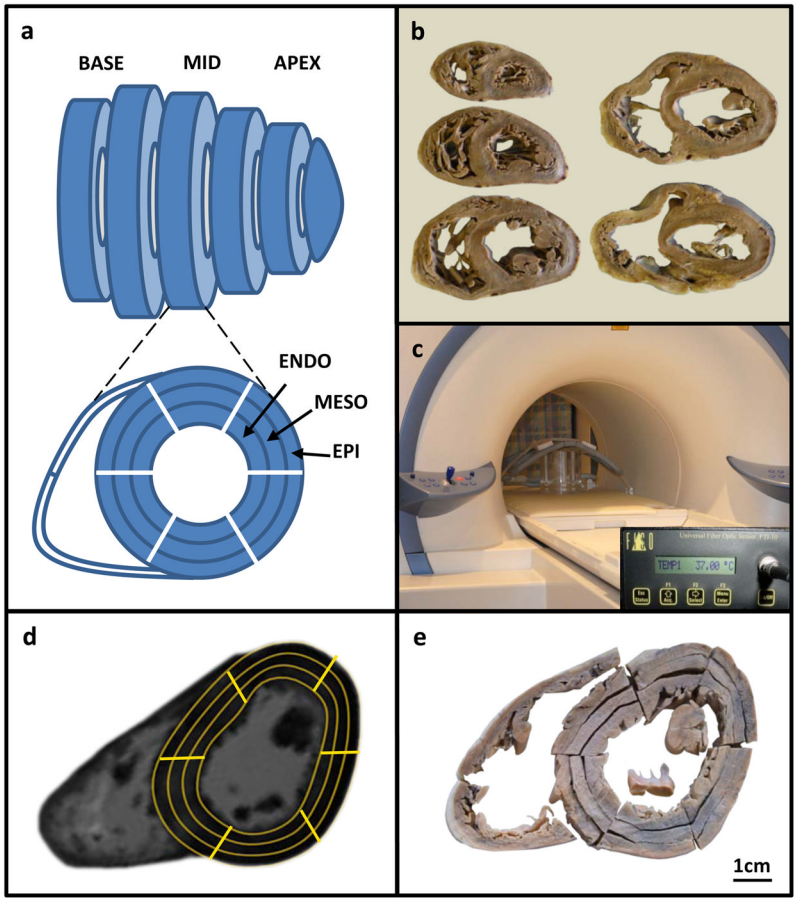

Figure 1.
Experimental setup.
A) Diagram of short-axis cardiac slices showing regions of interest (ROIs); B) Set of slices from a single heart; C) Slices inside scanner; D) Ex-vivo CMR image with ROIs used to determine T2* decay; E) Identical slice with segmentation performed to correspond with ROIs used for T2* measurement.

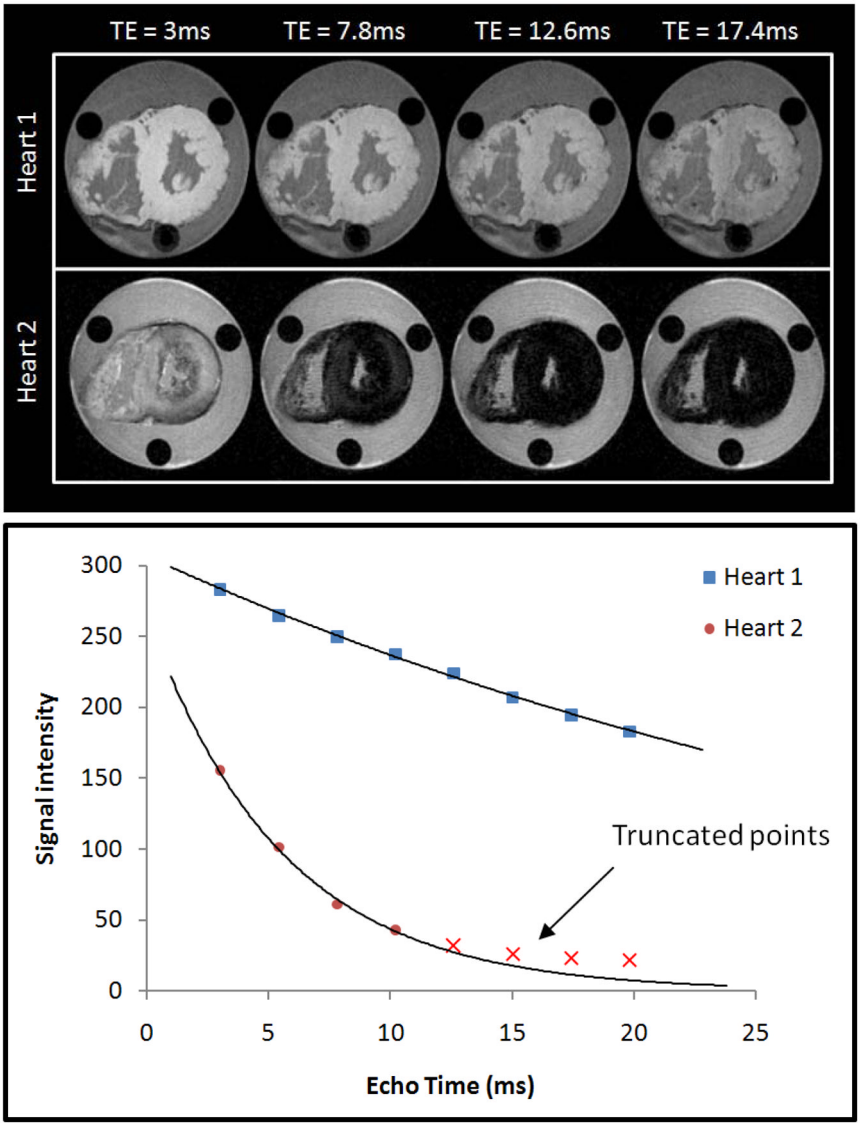

Figure 2.

Example of ex-vivo cardiac T2* scans.

Representative images of two hearts are shown at increasing echo times (TE) from 3ms to 17.4ms. Heart 1 has normal iron levels and remains bright whereas heart 2 (which has severe iron loading) shows progressive darkening with increasing echo time. The graph shows signal intensity (arbitrary units) plotted against echo time (ms) for the hearts in upper panel. Heart 1 has a shallow decay curve with T2* value of >20ms. Heart 2 has a much more rapid decay with T2* <10ms.

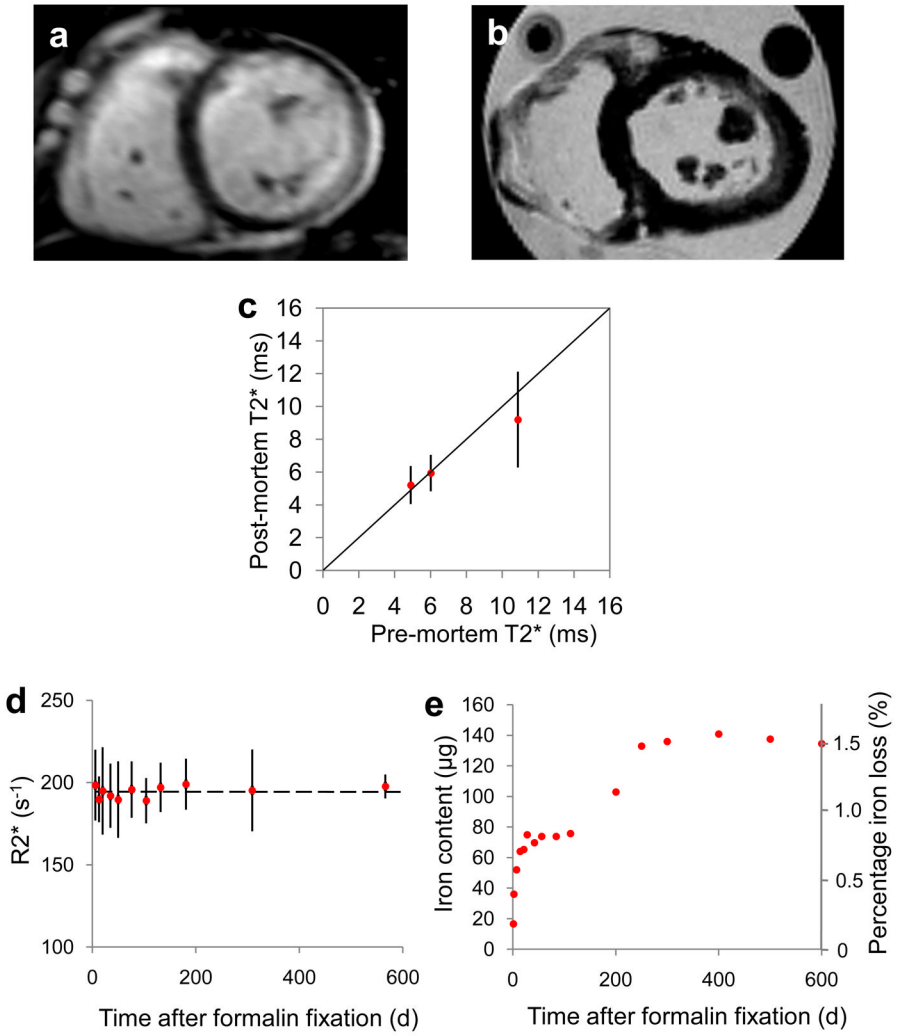

Figure 3.

Pre and post-mortem scans.

A) A pre-mortem mid-ventricular slice and B) the corresponding post-mortem slice of the same heart at the same position; C) Relationship between pre- and post-mortem T2* values measured from corresponding regions of interest in the mid-ventricular septum. Error bars represent standard deviation and the line of identity is given; D) R2* values measured from a single myocardial slice stored in formalin over a prolonged duration showing no significant change in R2*. The dashed line represents mean R2* ($194.4s^{-1}$) and error bars are ±SD; E) Iron content of the formalin solution in which a piece of myocardial tissue was stored, showing an initial rapid increase in iron which reaches a plateau after the first 300 days. There is an early and a late plateau, possibly suggesting a two-stage process of iron release, however no further iron appears to be lost after the first 300 days. Note that T2* (decay constant in milliseconds) is in widespread use for clinical iron assessment and is shown for the patient scan results, but that R2* (transverse relaxation rate in s^{-1}) has been used to compare measurements in post-mortem hearts as it has a more linear relation to iron concentration.

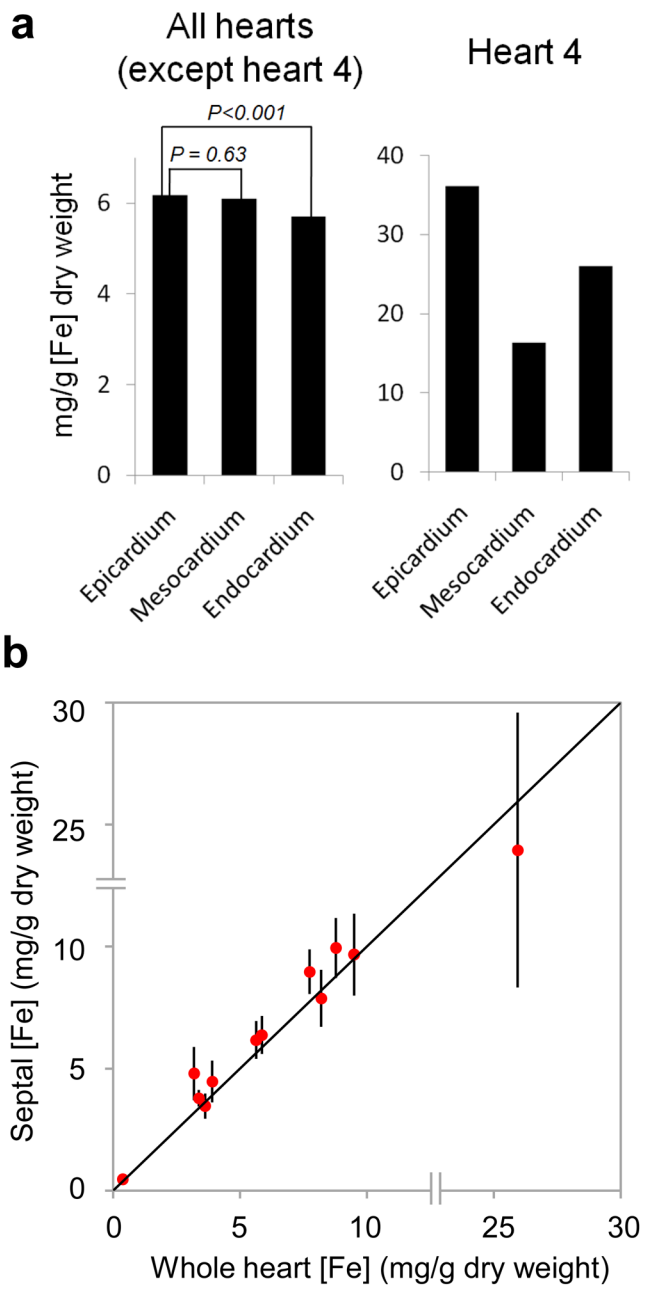

Figure 4.
Myocardial iron distribution.
A) Histogram showing transmural gradient across the LV myocardium; B) Graph of mid-septal iron concentration versus mean whole-heart iron concentration for each of the 12 hearts (data points are plotted against the line of identity, and error bars are ±SD of the septal samples). The double lines across each axis represent a discontinuity in the scale between 15 and 25mg/g for illustrative purposes.

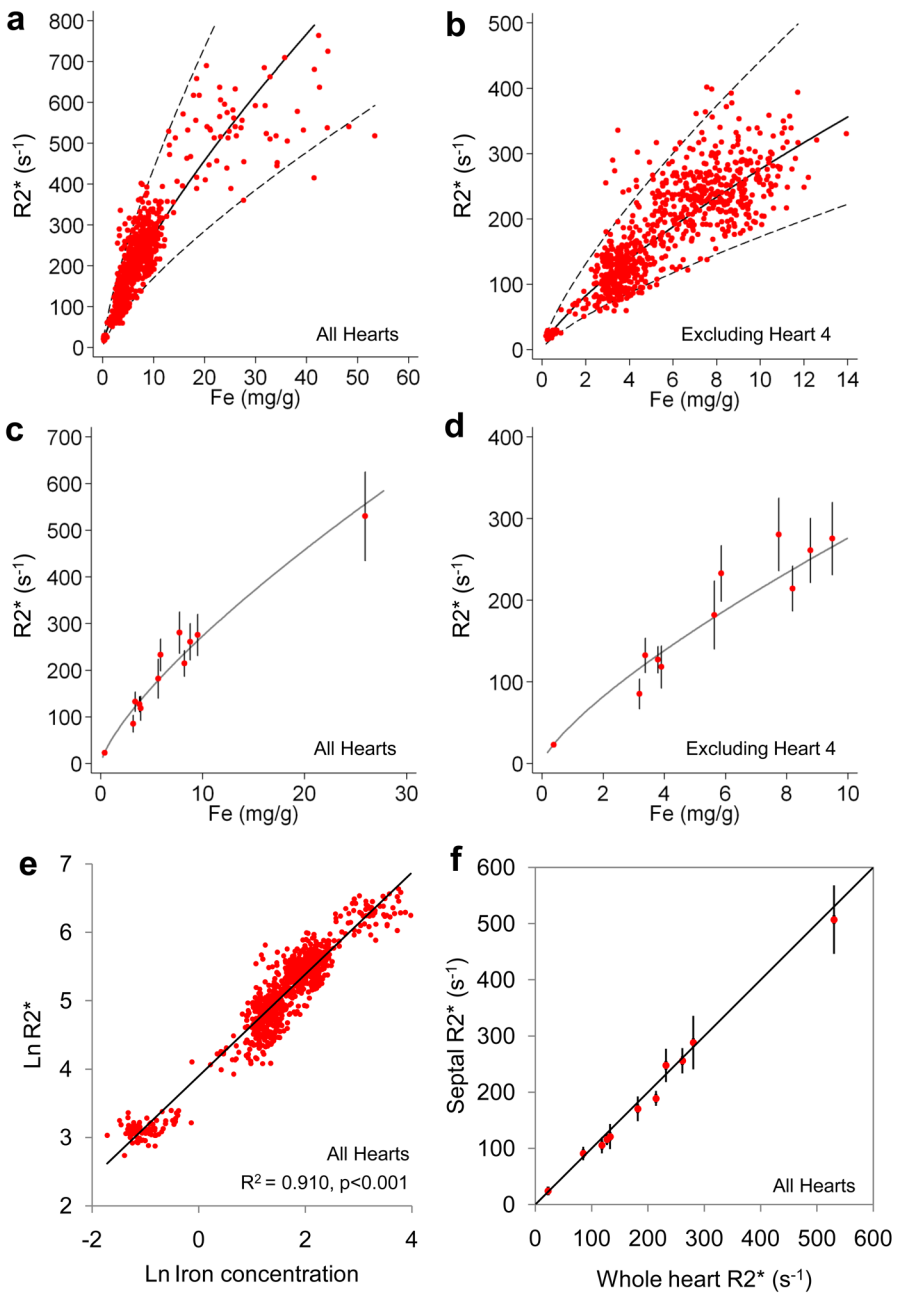

Figure 5.

Calibration of CMR versus myocardial iron concentration.

A) R2* plotted against myocardial iron concentration measured from each myocardial ROI. The regression (solid line) and 95% confidence bands (dotted lines) are shown and derived from analysis of the log-log data shown in figure 5E.; B) R2* versus myocardial iron concentration excluding heart 4. The regression (solid line) and 95% confidence bands (dotted lines) are shown and derived from analysis of the log-log data shown in figure 5E; C) Mean R2* plotted against mean iron concentration for each heart. The regression (solid line) is derived from analysis of the log-log data shown in figure 5E; D) Mean R2* versus mean iron concentration excluding heart 4. The regression (solid line) is derived from analysis of the log-log data shown in figure 5E; E) ln(R2*) plotted against ln([Fe]) for all

ROIs, including heart 4 showing the best fit linear regression line; F) Mean mid-septal R2* versus mean whole-heart R2* plotted against the line of identity, showing that the septal R2* value is highly representative of the whole-heart R2* (only 11 hearts are shown because severe artefact prevented analysis of mid-septal T2* in one heart).

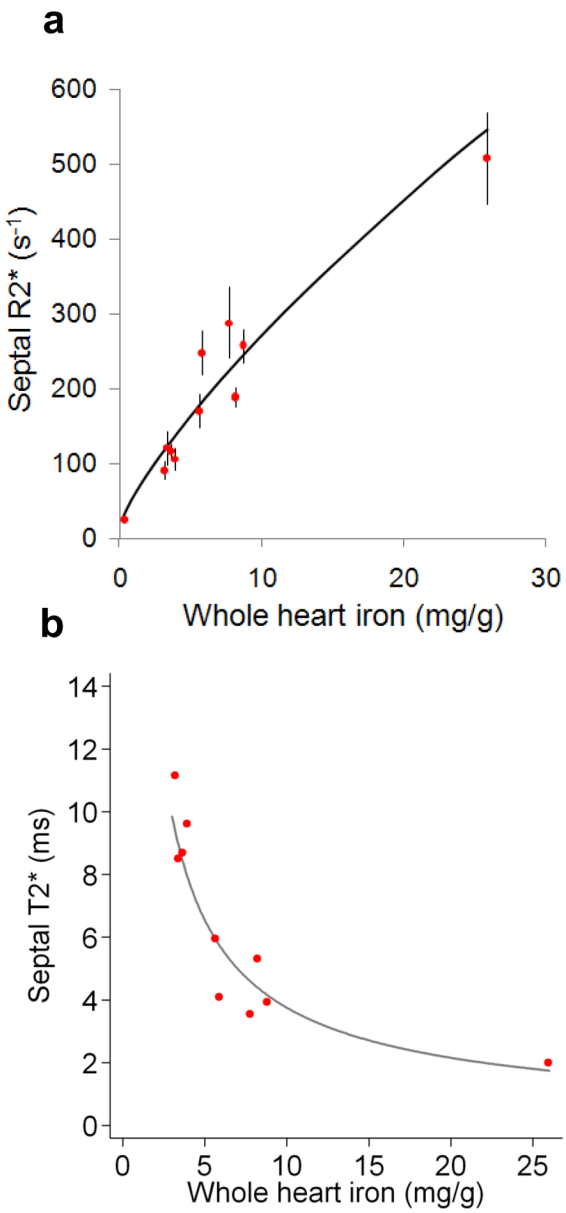

Figure 6.

Septal CMR measurements versus myocardial iron concentration.

A) Mean septal R2* plotted against mean iron concentration for each heart. Error bars are ±SD for septal R2* and the regression line is shown based on the log-log data shown in figure 5E. B) Mean septal T2* plotted against mean iron concentration for each heart. These two graphs illustrate the difference between T2* and R2* when compared to tissue iron. T2* shortens with increased iron concentration and hence its reciprocal R2* rises with tissue iron. T2* is used for clinical assessment of cardiac iron for historical reasons.

Table 1

Patient characteristics and clinical information.

Patient	Sex	Diagnosis	Death or cardiac transplantation	Age at death or transplantation	Cause of death or indication for transplant	LV [Fe] [mg/g dw] (mean ±SD)	Variability of [Fe] (CoV %)	Global Myocardial T2* [ms] (mean±SD)	Total estimated units transfused	Age started chelation (years)	Compliance
1	M	TM	Death	46	Ischemic stroke (no cardiac failure)	0.38±0.13	21.1	44.4±5.3	1584	6	Excellent
2	F	SA	Death	62	Cardiac failure	8.20±1.44	15.9	4.7±0.6	2000	42	Good
3	M	TM	Death	10	Cardiac failure	9.50±1.88	9.2	3.7±0.6	170	N/A[#]	N/A
4	F	TM	Death	15	Cardiac failure	25.9±10.3	17.6	2.0±0.4	288	N/A[†]	N/A
5	F	TM	Death	20	Cardiac failure	7.74±1.51	16.4	3.6±0.5	432	6	Poor
6	M	TM	Transplant	23	Cardiac failure	3.63±0.82	18.0	8.0±1.0	765	10	Not known
7	M	TM	Transplant	24	Cardiac failure	3.38±0.53	10.0	7.7±1.2	528	6	Good
8	M	TM	Transplant	21	Cardiac failure	5.87±1.0	9.5	4.4±0.6	500	4	Not known
9	F	TM	Transplant	31	Cardiac failure	8.78±1.88	10.5	3.9±0.6	624	7	Poor
10	M	TM	Death	24	Cardiac failure & mucormycosis	5.64±1.36	17.3	5.8±1.4	660	10	Poor
11	M	TM	Death	44	Cardiac failure	3.19±1.02	26.6	12.3±2.6	1209	18	Poor
12	M	DBA	Death	22	Cardiac failure & pneumonia	3.91±0.86	10.1	8.8±1.8	442	10	Poor

SD =standard deviation; LV =left ventricle; [Fe] =myocardial iron concentration; TM =Beta thalassemia major; SA =Sideroblastic anemia; DBA =Diamond Blackfan anemia; CoV =Coefficient of variation; N/A =not applicable (patients 3 and 4 did not receive iron chelation therapy)

[#]died 1964;

[†]died 1972.

Table 2

Distribution of iron throughout the left ventricular myocardium. The differences in iron concentration (Δ) are compared against the mean [Fe] dw for a reference (ref) region.

			All hearts (excluding heart 4)				Heart 4 alone			
LV Region of interest			[Fe] mg/g	95% CI		p value	[Fe] mg/g	95% CI		p value
Epicardium (reference)			6.17	4.65	7.69	Ref	36.10	31.58	40.62	Ref
Mesocardium (Δ)			−0.07	−0.34	0.20	0.63	−19.75	−21.71	−17.79	<0.001
Endocardium (Δ)			−0.46	−0.73	−0.19	0.001	−10.11	−12.75	−7.46	<0.001
Global LV (reference)			6.01	4.30	7.72	Ref	26.15	23.31	28.99	Ref
Basal	**1**	**Ant (Δ)**	−0.37	−1.30	0.56	0.43	1.12			
	2	**Ant-sep (Δ)**	0.09	−0.84	1.02	0.85	−7.31			
	3	**Inf-sep (Δ)**	−0.27	−1.20	0.66	0.57	−6.59			
	4	**Inf (Δ)**	−0.41	−1.34	0.52	0.39	5.26			
	5	**Inf-lat (Δ)**	−0.14	−1.07	0.79	0.77	−4.09			
	6	**Ant-lat (Δ)**	0.38	−0.55	1.31	0.43	−2.99			
Mid	**7**	**Ant (Δ)**	0.03	−0.90	0.96	0.94	4.39			
	8	**Ant-sep (Δ)**	0.50	−0.43	1.43	0.29	3.05			
	9	**Inf-sep (Δ)**	0.59	−0.34	1.52	0.22	−1.33			
	10	**Inf (Δ)**	−0.01	−0.94	0.92	0.98	−0.67			
	11	**Inf-lat (Δ)**	0.02	−0.91	0.95	0.97	2.23			
	12	**Ant-lat (Δ)**	0.43	−0.50	1.36	0.37	1.06			
Apical	**13**	**Ant (Δ)**	0.08	−0.85	1.01	0.87	4.88			
	14	**Sep (Δ)**	−0.29	−1.22	0.64	0.54	−4.43			
	15	**Inf (Δ)**	−0.12	−1.05	0.81	0.81	8.57			
	16	**Lat (Δ)**	−0.50	−1.43	0.43	0.29	3.69			
Global LV (reference)			5.99	4.28	7.71	Ref	26.15	23.31	28.99	Ref
Anterior (Δ)			−0.07	−0.93	0.78	0.87	3.46	−5.30	12.23	0.39
Anterolateral (Δ)			0.16	−0.70	1.01	0.72	−0.36	−8.30	7.58	0.93
Inferolateral (Δ)			−0.06	−0.91	0.80	0.89	1.56	−6.38	9.50	0.69
Inferior (Δ)			−0.16	−1.02	0.69	0.71	4.39	−3.31	12.09	0.26

	All hearts (excluding heart 4)				Heart 4 alone			
LV Region of interest	**[Fe] mg/g**	**95% CI**		**p value**	**[Fe] mg/g**	**95% CI**		**p value**
Inferoseptal (Δ)	−0.06	−0.92	0.79	0.89	−3.93	−7.39	−0.48	0.28
Anteroseptal (Δ)	0.20	−0.66	1.05	0.65	−5.11	−8.29	−1.93	0.16
Apical (Δ)	0.27	−0.55	1.10	0.51	1.99	−4.41	8.40	0.49
Mid (Δ)	−0.17	−1.00	0.66	0.69	0.44	−7.18	8.06	0.88
Basal (Δ)	−0.11	−0.93	0.72	0.80	−2.43	−9.30	4.44	0.40

AHA segments are numbered and labelled as: ant = anterior; sep = septum; lat = lateral; inf = inferior).

Circulation. Author manuscript; available in PMC 2012 September 07.

Table 3

Distribution of iron in the right ventricle, atria and valves. The differences in iron concentration (Δ) are compared against the mean LV [Fe] dw.

		All hearts (excluding heart 4)				Heart 4 alone			
	Region of interest	**[Fe] mg/g**	**95% CI**		**p value**	**[Fe] mg/g**	**95% CI**		**p value**
Right Ventricle	**Global LV [Fe] (reference)**	5.98	4.52	7.45	Ref	26.15	23.31	28.99	Ref
	RV Posterior (Δ)	−1.26	−1.75	−0.78	<0.001	2.55	−3.86	8.96	0.68
	RV Anterior (Δ)	−1.31	−1.80	−0.83	<0.001	10.50	5.51	15.50	0.10
	Global LV [Fe] (reference)	5.98	4.52	7.45	Ref	26.15	23.31	28.99	Ref
	Apical (Δ)	−0.98	−1.57	−0.39	0.001	6.73	6.59	6.95	0.38
	Mid (Δ)	−1.43	−2.02	−0.84	<0.001	7.16	−0.69	15.00	0.35
	Basal (Δ)	−1.45	−2.04	−0.86	<0.001	5.69	−10.07	21.45	0.46
Atria and valves	**Global LV [Fe] (reference)**	5.98	4.57	7.39	Ref	26.15	23.31	28.99	Ref
	LA anterior (Δ)	−0.78	−1.64	0.09	0.080	45.92			
	LA posterior (Δ)	−1.68	−2.59	−0.76	<0.001	13.26			
	LA lateral (Δ)	−1.11	−1.98	−0.24	0.013	30.81			
	Atrial septum (Δ)	−2.99	−3.86	−2.12	<0.001	20.81			
	RA anterior (Δ)	−3.28	−4.15	−2.41	<0.001	34.22			
	RA posterior (Δ)	−3.41	−4.28	−2.54	<0.001	22.17			
	RA lateral (Δ)	−3.09	−3.95	−2.22	<0.001	23.39			
	Aortic valve (Δ)	−4.45	−5.57	−3.33	<0.001	42.60			
	Mitral valve (Δ)	−4.37	−5.23	−3.50	<0.001	52.49			
	Pulmonary valve (Δ)	−4.33	−5.45	−3.21	<0.001	41.12			
	Tricuspid valve (Δ)	−4.40	−5.26	−3.53	<0.001	52.35			